Macromolecules

ARTICLE

pubs.acs.org/Macromolecules

In Situ ^{1}H NMR Studies of High-Temperature Nitroxide-Mediated Polymerization of *n*-Butyl Acrylate

Lebohang Hlalele[†] and Bert Klumperman*[,†,‡]

[†]Department of Chemistry and Polymer Science, University of Stellenbosch, Private Bag X1, Matieland 7602, South Africa

[‡]Laboratory of Polymer Chemistry, Eindhoven University of Technology, P.O. Box 513, 5600 MB Eindhoven, The Netherlands

ABSTRACT: This paper presents results on the independence of the rate of polymerization of *n*-butyl acrylate (*n*-BA) toward initial concentration of the alkoxyamine initiator. The alkoxyamine, 2-methyl-2-[*N*-*tert*-butyl-*N*-(1-diethoxyphosphoryl-2,2-dimethylpropyl)aminooxy]propionic acid (MAMA-DEPN), was used to initiate and mediate the polymerization of *n*-BA in the temperature range 90−120 °C. *In situ* ^{1}H NMR spectroscopy was used to follow the consumption of the monomer and monitor other related reactions. Intra- and intermolecular chain transfer processes are well-known phenomena in the polymerization of *n*-BA that result in the transformation of secondary propagating radicals (SPRs) into tertiary midchain radicals (MCRs). At high polymerization temperature ($T \geq 110$ °C), the MCRs undergo β-fragmentation. The concentrations of the products of the β-fragmentation process (in the form of chains bearing 1,1-disubstituted alkene end group) were measured as a function of polymerization time. The independence of rate of polymerization of *n*-BA initiated by MAMA-DEPN can be explained in terms of thermal autoinitiation in the case where free $[DEPN]_0$ is no larger than 1 mol % relative to $[MAMA\text{-}DEPN]_0$.

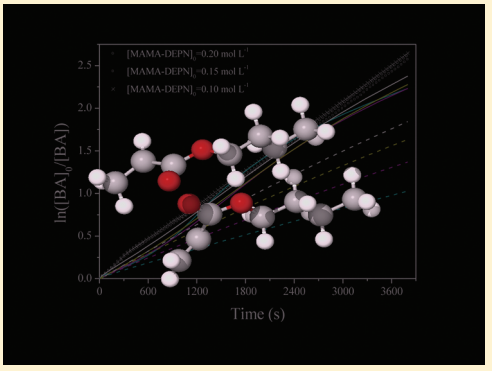

INTRODUCTION

Acrylate type monomers show more complex behavior in their polymerization mechanistic and kinetic features than other vinyl monomers such as styrene. Deviations from ideal behavior with respect to polymerization kinetics have previously been reported in the literature, with monomer reaction orders ranging from 1.4 to 1.8.[1] *n*-BA can undergo chain transfer to monomer and/or polymer. The former restricts the molar mass, and the latter results in branched polymer structures. Chain transfer to polymer can occur either intermolecularly or intramolecularly.[1] Intermolecular chain transfer involves transfer of a radical reactive site from a chain-end position of a growing polymer chain to a midchain position of another polymer chain by hydrogen abstraction.

Intramolecular chain transfer (so-called backbiting) occurs by hydrogen abstraction from a unit in proximity (the antepenultimate unit) of the propagating radical, via the formation of an intermediate six-membered ring structure (Scheme 1).[2] Intramolecular chain transfer is governed by the rate coefficient of backbiting (k_{bb}). It should, however, be noted that intramolecular chain transfer can occur at any position along the polymer backbone with slightly different governing rate coefficients. However, the most probable and more favored position is on the third unit from the chain-end radical.[2] Thus, k_{bb} can be assumed within good approximation as the only rate coefficient of intramolecular chain transfer. The result of the chain transfer to polymer process is the transformation of secondary propagating radicals (SPRs) into tertiary midchain radicals (MCRs). Intramolecular chain transfer has been reported as the main cause for the branched structure of poly(*n*-BA) prepared via nitroxide-mediated polymerization in bulk and miniemulsion polymerization.[3]

The MCRs exhibit a higher level of stability relative to the SPRs and as a result tend to add monomer at a rate an order of magnitude lower than the rate at which monomer is added to the SPRs.[4,5] Thus, due to the chain transfer process and the possible reaction pathways the MCRs can undergo (Scheme 2), the result is a system with two distinct coexisting transient radical species. The reaction pathways (Scheme 2) that will determine the fate of MCRs include (i) addition of monomer to the MCR (which will transform the MCRs to SPRs with a short branch chain) at a rate determined by k_p^t, (ii) β-fragmentation, which will result in the formation of an SPR and a chain bearing a 1,1-disubstituted alkene end group at a rate determined by the rate coefficient of β-fragmentation (k_β), and (iii) termination with either an SPR or another MCR at rates governed by k_t^t and k_t^{tt}, respectively.[4,6−8]

Nikitin and Hutchinson[4,9,10] derived analytical expressions to describe rate parameters in the polymerization of acrylate type monomers. These expressions are based on the assumption that β-fragmentation of the MCRs is a negligible process. The β-fragmentation process can be safely assumed negligible at low to moderate polymerization temperatures. However, at high polymerization temperature ($T \geq 110$ °C), β-fragmentation can no longer be considered negligible; thus, great care should be

Received: May 28, 2011
Revised: August 9, 2011
Published: August 25, 2011

Scheme 1. Intramolecular Chain Transfer to Polymer via the 1,5-Hydrogen Shift from the Antepenultimate Unit Resulting in the Transformation of a Secondary Propagating Radical (SPR) into a Midchain Radical (MCR) at a Rate Determined by the Rate Coefficient of Backbiting (k_{bb}) with "-Bu" Representing the *n*-Butyl Group

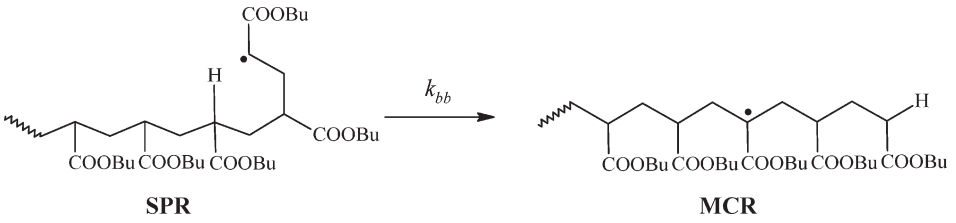

Scheme 2. Formation of Midchain Radicals (MCRs) from Secondary Propagating Radicals (SPRs) via Backbiting and the Subsequent Transformation of the MCR to SPR via β-Fragmentation and Monomer Addition

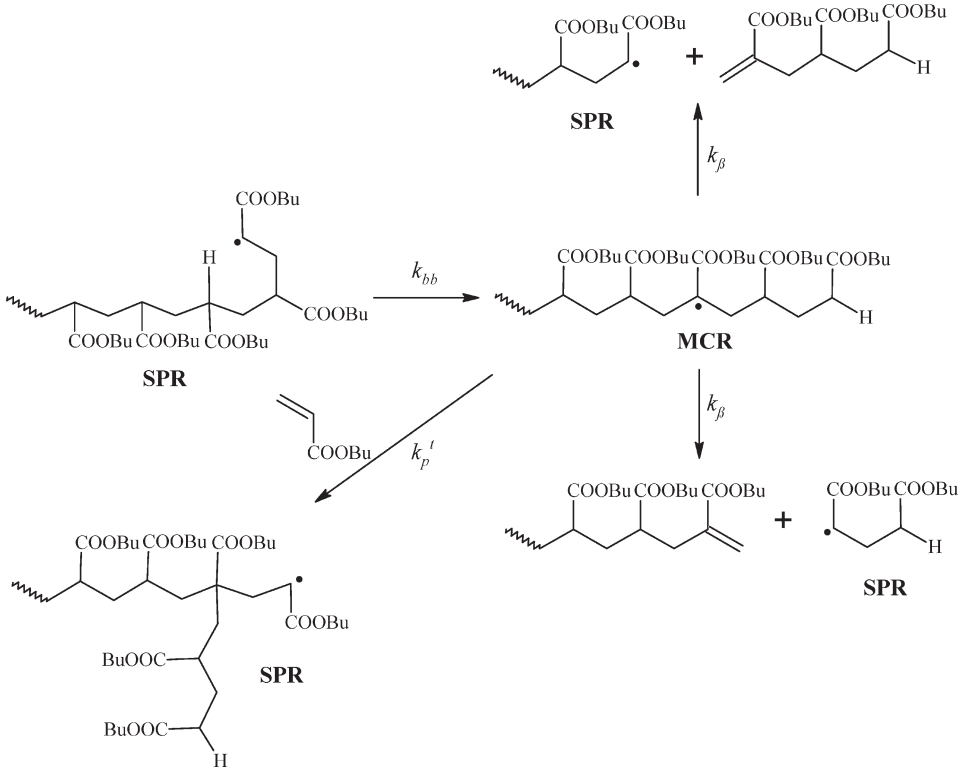

exercised in the use of such expressions. Koo et al.[11] reported the existence of β-fragmentation products at polymerization temperatures below 100 °C. Roos et al.[12] and Ahmad et al.[13] have shown the existence of branched structures in high and low molar mass poly(*n*-BA), respectively. The extent of branching can be related to the degree to which propagation of the MCR occurs, in addition to the branches formed from termination reactions of the SPR and MCR.

In the present work, ^{1}H NMR spectroscopy was used as a tool to probe the kinetics of *n*-BA polymerization. Recently, *in situ* ^{1}H NMR spectroscopy has proven to be a very useful and powerful technique in investigations of controlled/living radical polymerization.[14] Conversion vs time plots for *n*-BA polymerizations initiated by 2-methyl-2-[*N*-*tert*-butyl-*N*-(1-diethoxyphosphoryl-2,2-dimethylpropyl)aminooxy]propionic acid (MAMA-DEPN, also known as BlocBuilder, Figure 1) were found in this work to be independent of the initial alkoxyamine concentration within the range of initiator concentration studied. Why would

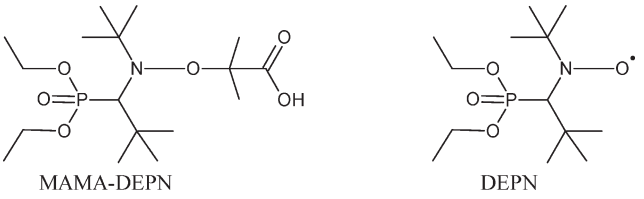

Figure 1. Structures of the alkoxyamine initiator (MAMA-DEPN) and the corresponding free nitroxide (DEPN).

the rate of polymerization of *n*-BA not increase with increasing concentration of the alkoxyamine initiator? To our knowledge, there has been no report in the literature addressing this question. Concentration profiles of the products of the β-fragmentation process (chains bearing unsaturated 1,1-disubstituted alkene end groups, i.e., macromers) are constructed at varying polymerization temperatures.

In this work no SEC data are included, since it is well accepted based on data in the literature[15−17] that the polymerization of *n*-BA using MAMA-DEPN follows the path of controlled/living radical polymerization, with a linear evolution of molecular weight with monomer conversion. It is also well-known that living radical polymerization processes that are allowed to proceed to very high conversion tend to lose their living character. Polymerization to high conversion in this particular case is important in the accumulation of the macromers as a function of both time and monomer conversion.

EXPERIMENTAL SECTION

Materials. The alkoxyamine MAMA-DEPN was synthesized following methods described in the literature.[18−21] *n*-BA (Plascon Research Center, University of Stellenbosch) was washed repeatedly with aqueous 10% NaOH and distilled deionized water to remove inhibitors, dried for several hours with anhydrous $MgSO_4$, and then distilled under vacuum and stored at low temperatures. Deuterated dimethyl sulfoxide (DMSO-d_6, Cambridge Isotope Laboratories, 99%) and dimethylformamide (DMF, Sigma-Aldrich) were used as received.

DEPN-Mediated Polymerization of *n*-BA Followed via *in Situ* ^{1}H NMR. A typical polymerization was conducted as follows: 302.1 mg of DMSO-d_6 (3.867 mmol), 30.7 mg of MAMA-DEPN (0.08048 mmol), 203.5 mg of *n*-BA (1.588 mmol), and 20 μL of DMF (internal reference) were thoroughly mixed and introduced into a J-Young type NMR tube. The sample was degassed by three freeze−pump−thaw cycles and backfilled with nitrogen gas. The ratio of the initial alkoxyamine concentration to the initial monomer concentration was high to limit the theoretical molecular weight below 5000 g mol^{-1} in some experiments, which afforded relative ease of end group detection by ^{1}H NMR spectroscopy. The ^{1}H NMR spectra were recorded on a 400 MHz Varian Unity Inova spectrometer. The ^{1}H NMR spectra were acquired with a 3 μs (40°) pulse width and a 4 s acquisition time. The NMR tube was first inserted into the magnet at 25 °C, the magnet fully shimmed on the sample, and a spectrum collected to serve as reference at 25 °C. This was followed by removal of the sample from the magnet after which the cavity of the magnet was heated to 120 °C and allowed to stabilize before reintroducing the sample into the cavity of the magnet. After the reinsertion of the sample, additional shimming was performed to acquire optimum conditions. The first spectrum was acquired 3−5 min after the reinsertion, followed by periodic spectra acquisition every 2 min for 60 min. The phase correction was performed automatically while baseline correction and integration of the spectra were carried out manually using ACD Laboratories 10.0 1D ^{1}H NMR processor. Concentration profiles were constructed relative to the reference (DMF).

The three monomer peaks in region "B" in Figure 2 were used to follow the concentration of the monomer during the polymerization of *n*-BA, and these peaks were integrated against the −CHO proton peak of DMF (reference) at ca. 7.95 ppm (labeled A in Figure 2). The enlarged region "B" of Figure 2, illustrating the monomeric protons responsible for the observed signals, is shown in Figure 3. The concentration of DMF remained constant throughout the entire polymerization time. With the concentration of all starting materials known (particularly the reference material), the actual concentration of all species during the polymerization could easily be deduced.

The fractional monomer conversion was calculated from the initial concentration of the monomer $[M]_0$ and the monomer concentration $[M]_t$ at time "t" during the polymerization according to the expression conversion = $([M]_0 - [M]_t)/[M]_0$, assuming that all monomer consumed is converted to polymer.

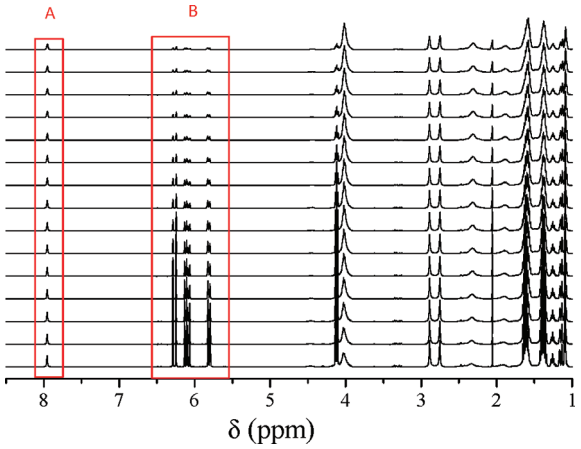

Figure 2. ^{1}H NMR spectra (δ in the range 1−8.5 ppm) at different times during the polymerization of *n*-BA at 120 °C initiated by MAMA-DEPN in DMSO-d_6. The region labeled "B" are peaks due to the vinyl protons of the *n*-BA monomer, and the peak labeled "A" is due to the −CHO proton of the reference, DMF. Spectra from bottom to top are measured between t = 8 min and t = 64 min, with a time interval of 4 min between consecutive spectra.

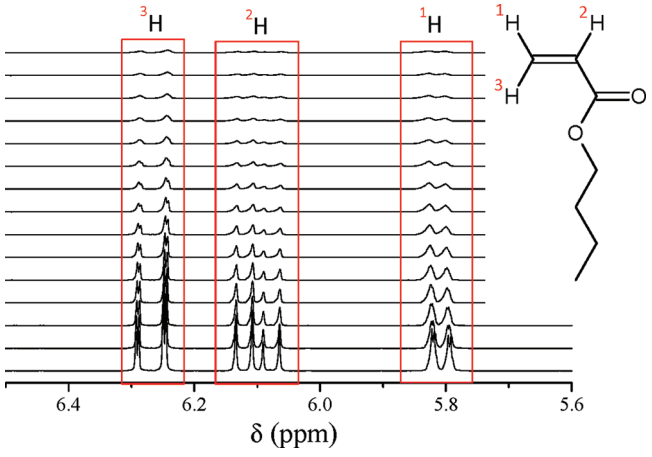

Figure 3. The enlarged version of the part labeled "B" in Figure 2 indicates the spectral region of the vinyl protons of the *n*-BA monomer, during the polymerization at 120 °C initiated by MAMA-DEPN in DMSO-d_6.

RESULTS AND DISCUSSION

The evolution of the conversion index with time in the polymerization of *n*-BA at different initial concentration of the alkoxyamine initiator is illustrated in Figure 4. An apparent independence of the rate of polymerization toward the initial concentration of the alkoxyamine is observed.

The independence of the rate of polymerization on the initial alkoxyamine concentration in the case of styrene has been extensively studied and is well reported in the literature.[22−27] In the case of styrene it is generally accepted that the apparent independence of the rate of polymerization as a function of initial concentration of the initiator can be explained by the significant thermal autoinitiation of styrene. Could the same explanation be applicable in the case of *n*-BA polymerization with MAMA-DEPN? If indeed thermal autoinitiation plays a role in the observed phenomenon, a possible route of proving this would involve conducting the polymerization at lower temperatures, resulting in a system with minimal contribution from thermal autoinitiation. Thus,

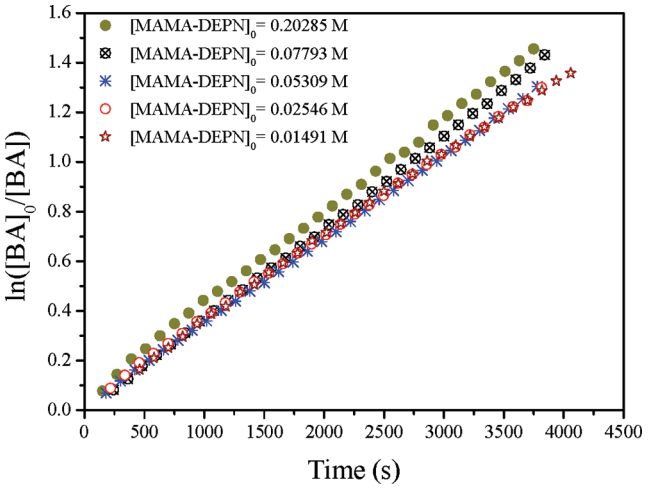

Figure 4. Conversion index plot for *n*-BA polymerization initiated with different initial alkoxyamine concentrations in DMSO-d_6 at 120 °C.

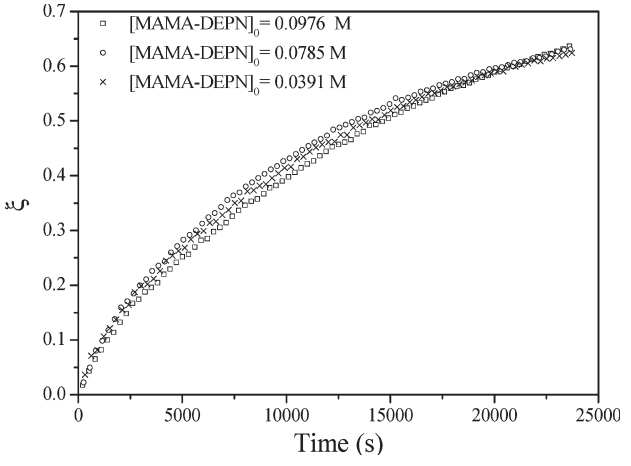

Figure 5. Conversion vs time plots for *n*-BA polymerization initiated with different initial alkoxyamine concentrations in DMSO-d_6 at 100 °C.

low-temperature experiments would allow for the effect due to the initial concentration of the alkoxyamine to be more pronounced in the kinetic profiles. The evolution of monomer conversion as a function of time for the polymerization of *n*-BA conducted at 100 °C (Figure 5) showed no apparent dependence on initial concentration of the alkoxyamine.

The consistency of the apparent independence of the rate of polymerization on alkoxyamine concentration within the temperature range studied does not provide conclusive evidence. It does not link the phenomenon unequivocally to thermal autoinitiation as in the case of styrene. With the observed independence of rate on initiator concentration, it was important to further quantitatively assess the possible contribution of thermal autoinitiation to the observed phenomenon. When neat *n*-BA was degassed and immersed in an oil bath at 120 °C, the system gelled within minutes, with similar results observed at 100 °C. However, in the presence of TEMPO (0.02 mol %) without initiator, no polymer formed even after 48 h at 100 °C. The C−ON bond between the *n*-BA derived radical and TEMPO would be expected to be stable enough to allow complete

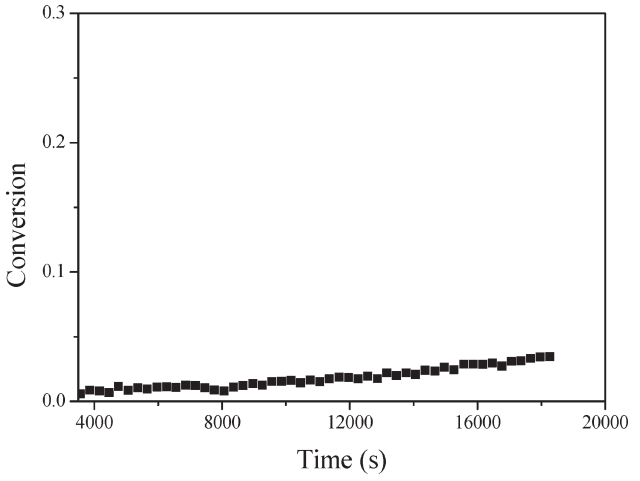

Figure 6. Evolution of *n*-BA conversion with time for thermally initiated polymerization in DMSO-d_6 in the presence of 5.30×10^{-2} mol L^{-1} free DEPN at 120 °C.

Scheme 3. Reaction Equations for Thermally Initiated *n*-BA (M) Polymerization in the Presence of Free Nitroxide (Y), Illustrating Thermal Initiation Step (1), Reversible Deactivation and Activation Steps (2 and 3), Propagation Step (4), and Termination Step (5)

$$2M \xrightarrow{k_{thrm}} 2P_1 \quad (1)$$

$$P_1 + Y \xrightarrow{k_c} P_1\text{-}Y \quad (2)$$

$$P_1\text{-}Y \xrightarrow{k_d} P_1 + Y \quad (3)$$

$$P_1 + M \xrightarrow{k_p} P_2 \quad (4)$$

$$P_1 + P_1 \xrightarrow{k_t} D \quad (5)$$

consumption of TEMPO by thermally initiated monomer derived radicals. The system would then be expected to behave as in the case of neat *n*-BA after all or most of the TEMPO has been consumed. On the basis of simulation results, it was expected that for the lowest concentration of TEMPO employed enough transient radical would be generated to fully consume TEMPO. Contrary to the expected results, in the entire TEMPO to *n*-BA mole ratios (0.02−1.5 mol % TEMPO relative to *n*-BA) studied no polymer formed. *In situ* ^{1}H NMR experiments were then conducted to follow in real time the rate of monomer consumption in the presence of DEPN without initiator at 120 °C

The experimental setup was similar to previously described *in situ* ^{1}H NMR homopolymerization of *n*-BA, with MAMA-DEPN replaced with DEPN. Evolution of the monomer conversion with polymerization time is shown in Figure 6, and only after ca. 2.5 h does significant monomer consumption occur.

To quantify the thermal autoinitiation of *n*-BA, Scheme 3 is considered. At early reaction times, reactions 4 and 5 from Scheme 3 can be considered negligible. Because of the large excess of free DEPN at these early reaction times, the thermally generated monomeric radicals (reaction 1) will react mainly according to reactions 2 and 3. In this time regime where

propagation and termination reactions are negligible, the rate of consumption of the monomer can be defined by eq 1, which upon integration yields eq 2.

$$d[M]/dt = -k_{thrm}[M]^2 \quad (1)$$

$$\frac{1}{[M]} - \frac{1}{[M]_0} = k_{thrm}t \quad (2)$$

A plot of the left-hand side of eq 2 with time yields a straight line (Figure 7) where the slope can be related to the rate coefficient of thermal autoinitiation in the case where propagation and termination reactions are negligible. Deviation from linearity signifies the occurrence of propagation and termination reactions. It should be noted that with longer polymerization times the decomposition of DEPN might play a role in the kinetics of the polymerization, but it is not expected to be significant in the analysis of thermal autoinitiation of *n*-BA. The data obtained via *in situ* ^{1}H NMR will be subject to scatter due to the minute difference in monomer concentration being measured; thus, care should be exercised in the treatment of data. The rate coefficient of thermal autoinitiation (k_{thrm} = 3.5 × 10^{-7} L mol^{-1} s^{-1} [R^2 = 0.87]) extracted from Figure 7 is in reasonable agreement with k_{thrm} = 1.578 × 10^{-7} L mol^{-1} s^{-1} determined from the Arrhenius parameters reported by Rantow et al.[8] at 120 °C.

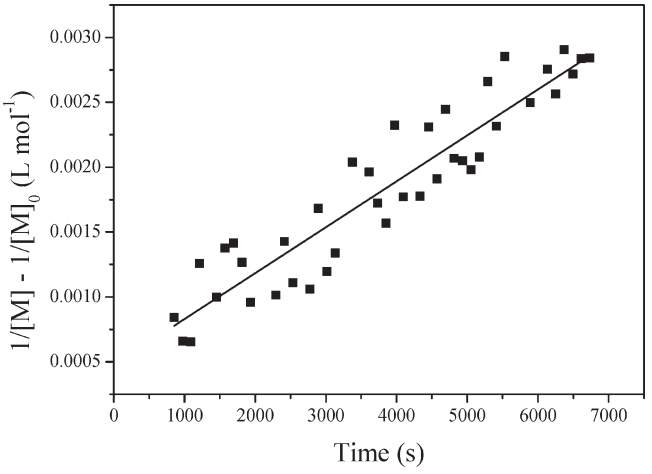

Figure 7. Plot of the negative inverse monomer consumption (■) with time in the linear range with the solid line as the linear fit to the data with a slope = k_{thrm} = 3.5 × 10^{-7} L mol^{-1} s^{-1} and R^2 = 0.87. [*n*-BA]$_0$ = 3.12 mol L^{-1} and [DEPN]$_0$ = 4.52 × 10^{-2} mol L^{-1} at 120 °C with DMSO-d_6 as the solvent.

The rate coefficient of thermal autoinitiation determined in this work at 120 °C is approximately an order of magnitude less than that of styrene.[28] To link together the observed experimental results (thermal autoinitiation and rate independence), simulation of *n*-BA polymerization was considered.

Modeling of high-temperature *n*-BA polymerization has proven to be quite a task due to the complicated mechanistic features of the system. Effects of thermal autoinitiation, equilibrium involving MCRs, and [DEPN]$_0$ (generated by decomposition at ambient temperatures) on the polymerization kinetics were investigated via modeling of the system using Predici software package. The simulations were carried out using Predici software package (version 6.72.3) in the moment mode. Residual orientated parameter estimation (PE, with automatic projection) studies with the Predici software package were then carried out to estimate the optimum values of k_c^t and k_d^t for which the model would fit the experimental data. The optimum values for the rate coefficients returned from the PE study are shown in Table 1.

The model implemented in the Predici software package for the *n*-BA polymerization is illustrated in Scheme 4, with all rate coefficients shown in Table 1. Because of the well-established chain transfer to polymer, the coexistence of two distinct types of transient radicals results in a system in which two equilibrium reactions should be considered.

The rate coefficients (k_c^t and k_d^t) describing the reversible deactivation−activation reaction between the nitroxide and the MCR were estimated via the parameter estimation tool of the Predici software package. The rate coefficients describing the NMP equilibrium for the *n*-BA/DEPN system reported in the literature were assumed to hold true in the description of the equilibrium involving the SPR. This assumption is not particularly true, as the equilibrium constant reported in the literature for this system is in actual fact a composite value within which the description of the two equilibria processes are embedded. The rate coefficient of first monomer addition ($k_{p,1}$) for the addition of *n*-BA to the 2-carboxyprop-2-yl radical is not known. This rate coefficient is however believed to be close to

Table 1. Rate Coefficients Used in the Kinetic Modeling of *n*-BA Using the Predici Simulation Package

	A	E_a (kJ mol^{-1})	value at 120 °C	refs
k_{act}	2.4 × 10^{14} s^{-1}	112.3	0.289 s^{-1}	29
k_{deact}			5.0 × 10^6 L mol^{-1} s^{-1}	16
$k_{p,1}$	4.0 × 10^6 L mol^{-1} s^{-1}	19.8	9.36 × 10^3 L mol^{-1} s^{-1}	30
k_p	2.31 × 10^7 L mol^{-1} s^{-1}	18.1	9.10 × 10^4 L mol^{-1} s^{-1}	31
k_c			2.80 × 10^7 L mol^{-1} s^{-1}	16, 32
k_d			1.55 × 10^{-3} s^{-1}	16
k_t			7.34 × 10^7 L mol^{-1} s^{-1}	16
k_{bb}	3.50 × 10^7 L mol^{-1} s^{-1}	29.3	4.48 × 10^3 L mol^{-1} s^{-1}	8
k_p^t	1.52 × 10^6 L mol^{-1} s^{-1}	28.9	2.20 × 10^2 L mol^{-1} s^{-1}	4
k_β	8.60 × 10^{10} L mol^{-1} s^{-1}	71.5	2.72 × 10^1 s^{-1}	1
k_c^t			1 × 10^6 L mol^{-1} s^{-1}	this work
k_d^t			5.32 × 10^{-2} s^{-1}	this work
k_t^t			3.90 × 10^7 L mol^{-1} s^{-1}	10
k_t^{tt}			2.80 × 10^6 L mol^{-1} s^{-1}	10
k_{thrm}			3.54 × 10^{-7} L mol^{-1} s^{-1}	this work

dx.doi.org/10.1021/ma201216e |*Macromolecules* 2011, 44, 7100–7108

Scheme 4. Nitroxide-Mediated *n*-BA Polymerization Model Implemented into Predici

R-Y			k_{act} →	R	+	Y
R	+	Y	k_{deact} →	R-Y		
2BA			k_{thrm} →	$2P_1$		
R	+	BA	$k_{p,1}$ →	P_1		
P_n	+	BA	k_p →	P_{n+1}		
P_n	+	Y	k_c →	P_n-Y		
P_n-Y			k_d →	P_n	+	Y
P_n			k_{bb} →	Q_n		
Q_n	+	BA	k_p' →	P_{n+1}		
Q_n			k_β →	P_m	+	$D^{=}_{n-m}$
Q_n	+	Y	k_c' →	Q_n-Y		
Q_n-Y			k_d' →	Q_n	+	Y
P_n	+	P_m	k_t →	D		
P_n	+	Q_m	k_t' →	D		
Q_n	+	Q_m	k_t'' →	D		

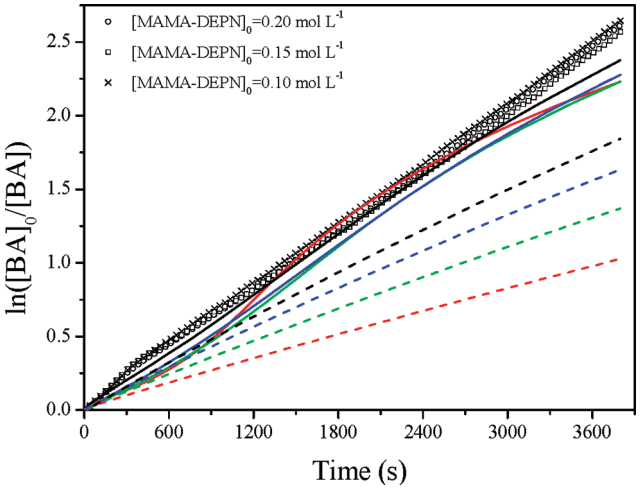

Figure 8. Simulated conversion index plots of *n*-BA polymerization at different initial concentration of the alkoxyamine (MAMA-DEPN) vs experimental data (○, □, and × in the legend). Simulated conversion index plots are illustrated by dashed lines (thermal autoinitiation excluded) and solid lines (thermal autoinitiation included) for $[n\text{-BA}]_0$ = 3.0 mol L^{-1}. The line colors red, green, blue, and black correspond to 0.05, 0.10, 0.15, and 0.20 mol L^{-1} of MAMA-DEPN, respectively.

that of addition of *n*-BA to 2-(alkoxy)carboxyprop-2-yl radical utilized in the model.[16]

Model vs experimental conversion index plots for *n*-BA polymerization at different initial concentration of the alkoxyamine are illustrated in Figure 8.

Deviation from linearity of the simulated plots in Figure 8 is due to the changing ratio of the MCR to SPR, which evolves with polymerization time. From Figure 8, it is apparent that, as in the case of styrene, thermal autoinitiation is the responsible factor for

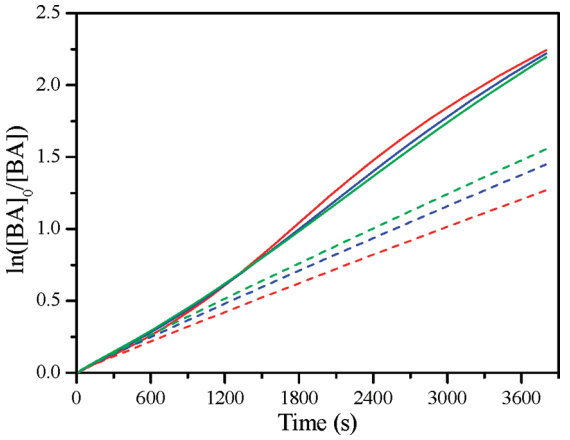

Figure 9. Simulated conversion index plots for *n*-BA in the presence of 1 mol % free DEPN relative to MAMA-DEPN added with thermal autoinitiation step taken into account (solid lines) and 1 mol % free DEPN relative to MAMA-DEPN added without thermal autoinitiation (dashed lines) for $[n\text{-BA}]_0$ = 3.0 mol L^{-1}. The colors red, blue, and green correspond to 0.10, 0.15, and 0.20 mol L^{-1} of MAMA-DEPN, respectively.

the observed phenomenon of rate independence. When thermal autoinitiation step is deactivated in the model, an increase in rate of polymerization is observed with increasing initial concentration of the alkoxyamine. Another matter of interest is the presence of free DEPN at the onset of polymerization and its effect on the kinetics. Alkoxyamines with high activation rate coefficients such as MAMA-DEPN are prone to spontaneous decomposition at ambient temperatures. The result of the decomposition is the presence of free DEPN at the onset of the reaction. As a result, the system is no longer a unimolecular NMP system. The effect of such free DEPN on the reaction kinetics is illustrated by Figure 9 (simulations).

In the presence of 1 mol % DEPN relative to $[\text{MAMA-DEPN}]_0$, the effect of the inclusion and exclusion of thermal autoinitiation step on reaction kinetics is summarized in Figure 9. The dependence of rate of polymerization on initiator concentration is observed with the exclusion of thermal autoinitiation (Figure 9, solid lines).

An assessment of the discrepancy of simulation data from experimental data could be used to estimate the concentration of initial free DEPN generated from spontaneous decomposition of MAMA-DEPN in this system. In absence of thermal autoinitiation step in the model, the experimentally obtained final conversion could not be obtained theoretically, highlighting the importance of such a reaction step. On the basis of the experimentally achieved overall concentration of the 1,1-alkene species and the monomer conversion, it can be argued in conjunction with simulation results that no more than 1 mol % free DEPN relative to $[\text{MAMA-DEPN}]_0$ is present at onset of polymerization in the system. This can be explained by the fact that, for simulations with greater than 1 mol % initial free DEPN, the achieved final monomer conversion and concentration of the 1,1-alkene species are well below those experimentally obtained.

Therefore, for such concentrations of free DEPN (<1 mol %), the independence of rate of polymerization has to rely largely on the thermal autoinitiation of *n*-BA (Figure 9). When the thermal autoinitiation step in the kinetic model is deactivated, with 1 mol % free DEPN present at polymerization onset, the rate of polymerization

dx.doi.org/10.1021/ma201216e |*Macromolecules* 2011, 44, 7100–7108

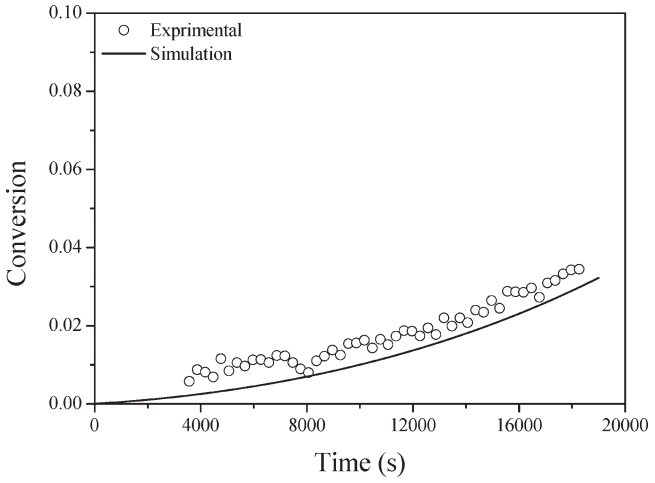

Figure 10. Simulated and experimental evolution of monomer conversion in thermally initiated *n*-BA polymerization in the presence of free DEPN. $[n\text{-BA}]_0 = 3.09$ mol L^{-1} and $[\text{DEPN}]_0 = 0.053$ mol L^{-1}.

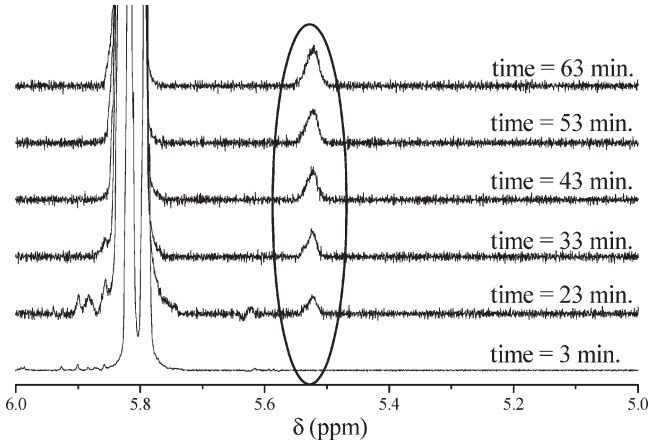

Figure 11. ^{1}H NMR spectra at the indicated reaction times illustrating the increasing intensity of the peak at around $\delta \sim 5.5$ ppm that is due to an increasing concentration of 1,1-disubstituted alkene end groups as a result of β-fragmentation of the MCRs in the polymerization of *n*-BA at 120 °C with $[\text{MAMA-DEPN}]_0 = 0.156$ mol L^{-1}, $[n\text{-BA}]_0 = 3.0$ mol L^{-1}, and DMSO-d_6 = 65% v/v.

is observed to increase with increasing concentration of the alkoxyamine (Figure 9).

The validity of the constructed polymerization model was further assessed by comparison of experimental data and simulated data for thermally initiated *n*-BA polymerization at 120 °C in the presence of free DEPN. Evolution of conversion as a function of time for a system with no radical initiator is illustrated in Figure 10. The sole mode of radical formation is by thermal autoinitiation of *n*-BA. Good agreement between the model and experimental data is observed, which further corroborates the model and the rate parameters used.

In addition to the regeneration of the SPR, β-fragmentation in *n*-BA polymerization also results in chains bearing the 1,1-disubstituted alkene end group (macromers). According to the work of Chiefari[33] on the synthesis of macromonomers via chain transfer to polymer, the 1,1-disubstituted alkene end group can be identified in a ^{1}H NMR spectrum by a signal at $\delta \sim 5.5$ ppm. A signal at $\delta \sim 5.5$ ppm assigned to one of the protons of the

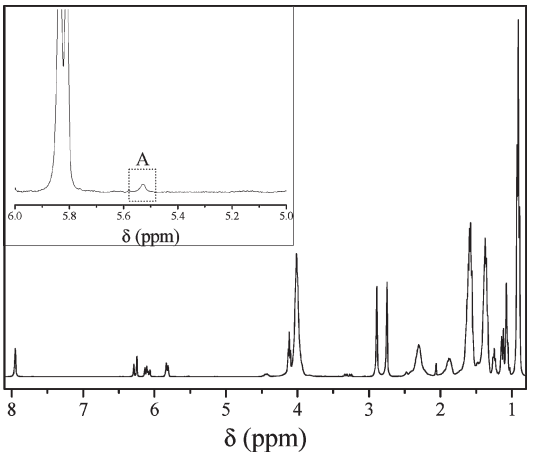

Figure 12. ^{1}H NMR spectrum taken after 2 h of polymerization of *n*-BA at 110 °C with $[\text{MAMA-DEPN}]_0 = 0.1494$ mol L^{-1}, $[n\text{-BA}]_0 = 3.0$ mol L^{-1}, and DMSO-d_6 = 65% v/v. The inset shows the expanded region in the range $6.0 > \delta$ (ppm) > 5.0 with the marked peak, labeled A, assigned to one of the protons of the 1,1-disubstituted alkene end group resulting from the β-fragmentation of the MCRs.

1,1-disubstituted alkene end group resulting from the β-fragmentation of the MCR, was observed to increase with polymerization time at 120 °C (Figure 11). The second peak expected at $\delta \sim 6.1$ ppm (due to the second vinyl proton of the 1,1-disubstituted alkene end group) could not be observed due to overlap with the signal of the monomer proton labeled ^{2}H in Figure 3.

The *n*-BA polymerizations initiated by MAMA-DEPN were also carried out at 90, 100, and 110 °C. A proton signal at $\delta \sim 5.5$ ppm was not observed at 90 and 100 °C, implying that the concentration of macromers was below the detection limit of the NMR spectrometer. However at 110 °C, the signal at $\delta \sim 5.5$ ppm was observed at high monomer conversion (Figure 12). At 110 °C, it can be postulated that these macromers accumulate with polymerization time and only at higher monomer conversion is the concentration of the species above the detection limit of the NMR instrument at experimental conditions.

Thus, Figures 11 and 12 indicate the existence of macromers at 120 and 110 °C, respectively. The absence of ^{1}H NMR evidence of such species at $T \leq 100$ °C is somewhat in contradiction with a few earlier studies in the literature[11,34,35] have reported the presence of macromers at temperatures lower than 100 °C. Evolution of the concentration of the macromers with polymerization time at 120 °C is illustrated in Figure 13. The concentration profile depicts that the overall rate of accumulation of the alkene bearing species is constant. The most likely explanation for the observed phenomenon is a constant rate of β-fragmentation. Alternatively, but less likely, the constant rate of accumulation of the macromers might be the result of a balance of two processes, namely the generation of the species and their incorporation in the growing polymer chain.[36,37] The implication of the latter process would be that, in addition to the formerly mentioned modes of generation of the MCRs, the incorporation of the macromers would also result in the formation of MCRs.

The concentration profiles of the macromers as a function of monomer conversion showed no dependence on the initial concentration of the alkoxyamine (Figure 14). This means that there is a constant rate of β-fragmentation, independent of initial alkoxyamine concentration. This observation is in agreement with the constant rate of polymerization as observed in Figure 4.

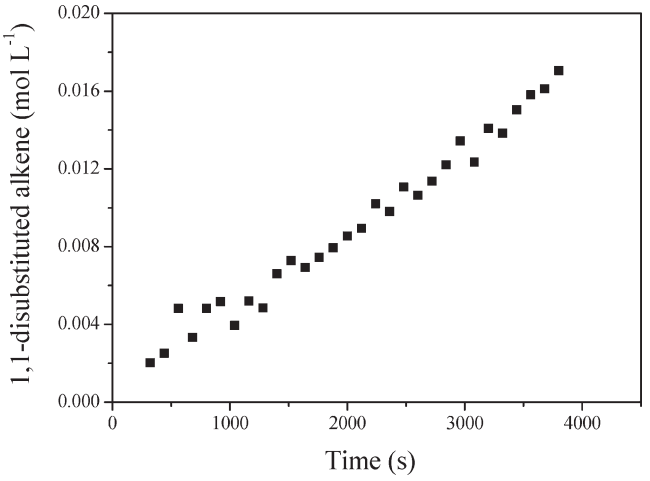

Figure 13. Evolution of concentration of 1,1-disubstituted alkene end group vs polymerization time during *n*-BA polymerization at 120 °C with $[\text{MAMA-DEPN}]_0$ = 0.156 mol L^{-1}, $[n\text{-BA}]_0$ = 3.0 mol L^{-1}, and DMSO-d_6 = 65% v/v.

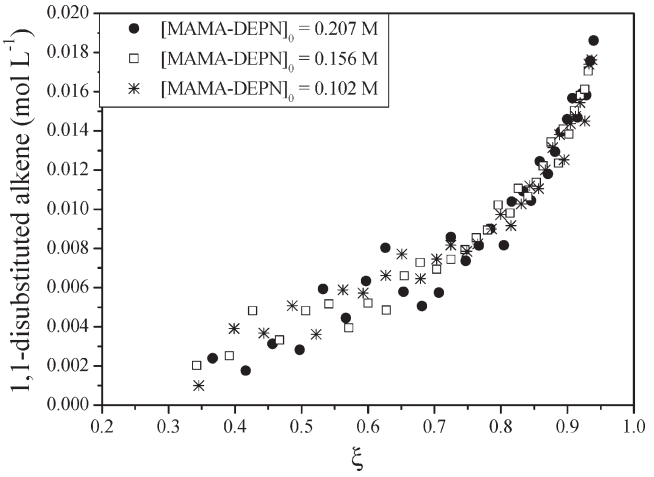

Figure 14. Evolution of relative concentration of 1,1-disubstituted alkene end group vs monomer conversion during *n*-BA polymerization at 120 °C for different initial concentrations of the alkoxyamine MAMA-DEPN. $[n\text{-BA}]_0$ = 3.0 mol L^{-1} and DMSO-d_6 = 65% v/v.

If the process of the incorporation of the 1,1-alkene species in the growing polymer is assumed negligible, the differential describing the concentration of the macromers with time can be expressed by eq 3, which upon integration yields eq 4.

$$\frac{\mathrm{d}[1,1\text{-alkene}]}{\mathrm{d}t} = k_\beta[\mathrm{Q}] \quad (3)$$

$$[1,1\text{-alkene}] = k_\beta[\mathrm{Q}]t \quad (4)$$

The linear evolution with time of the species bearing the 1,1-alkene end group as a result of β-fragmentation observed in Figure 13 is in agreement with the first-order dependence predicted by eq 4. The linear evolution can be used to approximate whether the incorporation of the macromers in the growing polymer is negligible or not. In the case where the incorporation of the macromers is significant, a deviation from linearity of the profile in Figure 13 would occur. The gradient of the linear plot in Figure 13 can be related to the concentration of the midchain radicals in the system with the knowledge of the β-fragmentation rate coefficient.

The constant rate of polymerization can be explained based on similar total concentration of transient radical irrespective of the initial concentration of the initiator as a result of thermal autoinitiation. On the other hand, this will lead to a constant concentration of MCRs and hence (at a fixed temperature) to a constant increase in the concentration of the macromers. Thus, the observed independence of the concentration of the macromers on the initial concentration of the alkoxyamine is a consequence of the similar rate of polymerization as observed in Figure 4.

CONCLUSION

The unimolecular nitroxide-mediated homopolymerization of *n*-BA using the alkoxyamine MAMA-DEPN has shown that the rate of polymerization is independent of the initial concentration of the alkoxyamine (within the concentration range studied). This phenomenon of the rate independence on initiator concentration has been explained in terms of the pronounced thermal autoinitiation in the polymerization of styrene. However, in the case of *n*-BA, where thermal initiation is not expected to be that significant, the issue of the rate independence has not been addressed in depth in the literature to date, to the best of our knowledge. The nature of the complexity of the system with two distinct coexisting transient radicals has complicated matters in the complete quest of understanding the kinetics and mechanistic features of acrylate type polymerization systems. The rate coefficient of thermal initiation of *n*-BA was determined as 3.5×10^{-7} L mol^{-1} s^{-1}, which is in good agreement with previously reported values. Through simulations, the effect of free DEPN on reaction kinetics with respect to the rate of polymerization was assessed. It can be concluded that at concentrations of 1 mol % free DEPN or less (relative to $[\text{MAMA-DEPN}]_0$) the independence of rate of polymerization of *n*-BA can be explained in terms of thermal autoinitiation. The concentration of chains bearing the 1,1-disubstituted alkene end was observed to increase linearly with time. It also showed no dependence on the initial concentration of the alkoxyamine, in agreement with the similar rates of polymerization observed.

AUTHOR INFORMATION

Corresponding Author

*E-mail: bklump@sun.ac.za.

ACKNOWLEDGMENT

The authors thank Jean McKenzie and Elsa Malherbe for assistance with *in situ* NMR reactions. Dr Michael Wulkow is acknowledged for his assistance with Predici simulations. Lebohang Hlalele also thanks Dr. E. T. A. van den Dungen for valuable discussions. The authors acknowledge financial suport from Stellenbosch University and from the SARChI initiative by the National Research Foundation (NRF) and the Department of Science and Technology (DST) of South Africa.

REFERENCES

(1) Junkers, T.; Barner-Kowollik, C. *J. Polym. Sci., Part A: Polym. Chem.* **2008**, *46*, 7585–7605.

(2) Dossi, M.; Storti, G.; Moscatelli, D. *Macromol. Symp.* **2010**, *289*, 119–123.
(3) Farcet, C.; Belleney, J.; Charleux, B.; Pirri, R. *Macromolecules* **2002**, *35*, 4912–4918.
(4) Nikitin, A. N.; Hutchinson, R. A.; Buback, M.; Hesse, P. *Macromolecules* **2007**, *40*, 8631–8641.
(5) Buback, M.; Hesse, P. *Polym. Prepr.* **2008**, *49* (2), 217–218.
(6) Junkers, T.; Koo, S. P. S.; Davis, T. P.; Stenzel, M. H.; Barner-Kowollik, C. *Macromolecules* **2007**, *40*, 8906–8912.
(7) Barth, J.; Buback, M.; Hesse, P.; Sergeeva, T. *Macromolecules* **2010**, *43*, 4023–4031.
(8) Rantow, F. S.; Soroush, M.; Grady, M. C.; Kalfas, G. A. *Polymer* **2006**, *47*, 1423–1435.
(9) Nikitin, A. N.; Hutchinson, R. A. *Macromolecules* **2005**, *38*, 1581–1590.
(10) Nikitin, A. N.; Hutchinson, R. A. *Macromol. Theory Simul.* **2006**, *15*, 128–136.
(11) Koo, S. P. S.; Junkers, T.; Barner-Kowollik, C. *Macromolecules* **2009**, *42*, 62–69.
(12) Roos, S. G.; Müller, A. H. E. *Macromol. Rapid Commun.* **2000**, *21*, 864–867.
(13) Ahmad, N. M.; Heatley, F.; Lovell, P. A. *Macromolecules* **1998**, *31*, 2822–2827.
(14) McLeary, J. B.; Calitz, F. M.; McKenzie, J. M.; Tonge, M. P.; Sanderson, R. D.; Klumperman, B. *Macromolecules* **2004**, *37*, 2383–2394.
(15) Nicolas, J.; Charleux, B.; Guerret, O.; Magnet, S. *Angew. Chem., Int. Ed.* **2004**, *43*, 6186–6189.
(16) Chauvin, F.; Dufils, P.-E.; Gigmes, D.; Guillaneuf, Y.; Marque, S. R. A.; Tordo, P.; Bertin, D. *Macromolecules* **2006**, *39*, 5238–5250.
(17) Phan, T. N. T.; Maiez-Tribut, S.; Pascault, J.-P.; Bonnet, A.; Gerard, P.; Guerret, O.; Bertin, D. *Macromolecules* **2007**, *40*, 4516–4523.
(18) Couturier, J. L.; Guerret, O.; Bertin, D.; Gigmes, D.; Marque, S.; Tordo, P. US20060142511, 2006 (assigned to Arkema, formerly Atofina, FR).
(19) Guerret, O.; Couturier, J.-L.; Le Mercier, C. US7126021, 2006 (assigned to Arkema, formerly Atofina, FR).
(20) Smith, L. I.; Emerson, O. H. *Org. Synth.* **1949**, *29*, 18–21.
(21) Talaty, E. R.; Boese, C. A.; Adewale, S. M.; Ismail, M. S.; Provenzano, F. A.; Utz, M. J. *J. Chem. Educ.* **2002**, *79* (2), 221–224.
(22) Catala, J. M.; Bubel, F.; Hammouch, S. O. *Macromolecules* **1995**, *28*, 8441–8443.
(23) Fukuda, T.; Terauchi, T.; Goto, A.; Ohno, K.; Tsujii, Y.; Miyamoto, T.; Kobatake, S.; Yamada, B. *Macromolecules* **1996**, *29*, 6393–6398.
(24) Gray, M. K.; Zhou, H.; Nguyen, S. T.; Torkelson, J. M. *Macromolecules* **2003**, *36*, 5792–5797.
(25) Greszta, D.; Matyjaszewski, K. *Macromolecules* **1996**, *29*, 5239–5240.
(26) Kruse, T. M.; Souleimonova, R.; Cho, A.; Gray, M. K.; Torkelson, J. M.; Broadbelt, L. J. *Macromolecules* **2003**, *36*, 7812–7823.
(27) Schulte, T.; Knoop, C. A.; Studer, A. *J. Polym. Sci., Part A: Polym. Chem.* **2004**, *42*, 3342–3351.
(28) Hui, A. W.; Hamielec, A. E. *J. Appl. Polym. Sci.* **1972**, *16*, 749–769.
(29) Bertin, D.; Gigmes, D.; Marque, S. R. A.; Tordo, P. *Macromolecules* **2005**, *38*, 2638–2650.
(30) Zytowski, T.; Knühl, B.; Fischer, H. *Helv. Chim. Acta* **2000**, *83*, 658–675.
(31) Barner-Kowollik, C.; Günzler, F.; Junkers, T. *Macromolecules* **2008**, *41*, 8971–8973.
(32) Chauvin, F.; Alb, A. M.; Bertin, D.; Tordo, P.; Reed, W. F. *Macromol. Chem. Phys.* **2002**, *203* (14), 2029–2041.
(33) Chiefari, J.; Jeffery, J.; Mayadunne, R. T. A.; Moad, G.; Rizzardo, E.; Thang, S. H. *Macromolecules* **1999**, *32*, 7700–7702.
(34) Junkers, T.; Bennet, F.; Koo, S. P. S.; Barner-Kowollik, C. *J. Polym. Sci., Part A: Polym. Chem.* **2008**, *46*, 3433–3437.
(35) Günzler, F.; Junkers, T.; Barner-Kowollik, C. *J. Polym. Sci., Part A: Polym. Chem.* **2009**, *47*, 1864–1876.
(36) Postma, A.; Davis, T. P.; Li, G.; Moad, G.; O'Shea, M. S. *Macromolecules* **2006**, *39*, 5307–5318.
(37) Sato, E.; Emoto, T.; Zetterlund, P. B.; Yamada, B. *Macromol. Chem. Phys.* **2004**, *205*, 1829–1839.